OXFORD

Loss of feedback regulation between FAM3B and androgen receptor driving prostate cancer progression

Tianfang Ma (iD), PhD,[1,2] Lianjin Jin, PhD,[1,2] Shanshan Bai, PhD,[1] Zhan Liu, PhD,[1] Shuo Wang, MD,[1,3] Beibei Shen, BS,[1,4] Yeyoung Cho, BS,[1,2] Subing Cao, PhD,[1] Meijuan J. S. Sun, PhD,[5] Ladan Fazli, MD,[6] David Zhang, [1,7] Chiyaro Wedderburn, BS,[1] Derek Y. Zhang, [1,8] Gavisha Mugon, BS,[5] Nathan Ungerleider, PhD,[9] Melody Baddoo, MS,[9] Kun Zhang, PhD,[10] Lovisa Holmberg Schiavone, PhD,[11] Brant R. Burkhardt, PhD,[12] Jia Fan, PhD,[5] Zongbing You, MD, PhD,[1,2] Erik K. Flemington, PhD,[9] Xuesen Dong, MD, PhD,[6] Yan Dong (iD), PhD[1,2,*]

[1]Department of Structural and Cellular Biology, Tulane University School of Medicine, Tulane Cancer Center, New Orleans, LA, USA
[2]Southeast Louisiana Veterans Health Care System, New Orleans, LA, USA
[3]Key Laboratory of Carcinogenesis and Translational Research (Ministry of Education), Urological Department, Peking University Cancer Hospital & Institute, Beijing, China
[4]Hubei Key Laboratory of Embryonic Stem Cell Research, Hubei University of Medicine, Shiyan, Hubei, China
[5]Department of Biochemistry and Molecular Biology, Tulane University School of Medicine, New Orleans, LA, USA
[6]Department of Urologic Sciences, Vancouver Prostate Centre, University of British Columbia, Vancouver, BC, Canada
[7]Duke University, Durham, NC, USA
[8]University of Southern California, Los Angeles, CA, USA
[9]Department of Pathology, Tulane University School of Medicine, Tulane Cancer Center, New Orleans, LA, USA
[10]Department of Computer Science, Bioinformatics Facility of Xavier RCMI Center of Cancer Research, Xavier University of Louisiana, New Orleans, LA, USA
[11]Discovery Biology, Discovery Sciences, R&D, AstraZeneca, Gothenburg, Sweden
[12]Department of Cell Biology, Microbiology and Molecular Biology, University of South Florida, Tampa, FL, USA

*Correspondence to: Yan Dong, PhD, Department of Structural and Cellular Biology, Tulane University School of Medicine, 1430 Tulane Avenue SL-49, New Orleans, LA 70112, USA (e-mail: ydong@tulane.edu).

Abstract

Background: Although the fusion of the transmembrane serine protease 2 gene (TMPRSS2) with the erythroblast transformation-specific-related gene (ERG), or TMPRSS2-ERG, occurs frequently in prostate cancer, its impact on clinical outcomes remains controversial. Roughly half of TMPRSS2-ERG fusions occur through intrachromosomal deletion of interstitial genes and the remainder via insertional chromosomal rearrangements. Because prostate cancers with deletion-derived TMPRSS2-ERG fusions are more aggressive than those with insertional fusions, we investigated the impact of interstitial gene loss on prostate cancer progression.

Methods: We conducted an unbiased analysis of transcriptome data from large collections of prostate cancer samples and employed diverse in vitro and in vivo models combined with genetic approaches to characterize the interstitial gene loss that imposes the most important impact on clinical outcome.

Results: This analysis identified *FAM3B* as the top-ranked interstitial gene whose loss is associated with a poor prognosis. The association between FAM3B loss and poor clinical outcome extended to fusion-negative prostate cancers where FAM3B downregulation occurred through epigenetic imprinting. Importantly, FAM3B loss drives disease progression in prostate cancer. FAM3B acts as an intermediator of a self-governing androgen receptor feedback loop. Specifically, androgen receptor upregulates FAM3B expression by binding to an intronic enhancer to induce an enhancer RNA and facilitate enhancer-promoter looping. FAM3B, in turn, attenuates androgen receptor signaling.

Conclusion: Loss of FAM3B in prostate cancer, whether through the TMPRSS2-ERG translocation or epigenetic imprinting, causes an exit from this autoregulatory loop to unleash androgen receptor activity and prostate cancer progression. These findings establish FAM3B loss as a new driver of prostate cancer progression and support the utility of FAM3B loss as a biomarker to better define aggressive prostate cancer.

The TMPRSS2-ERG fusion, which juxtaposes the *ERG* gene downstream of the androgen-responsive 5'-regulatory region of *TMPRSS2*, occurs in approximately 50% of prostate cancers (1). *TMPRSS2* and *ERG* are located approximately 2.8 megabases apart on chromosome 21. Approximately half of TMPRSS2-ERG fusions are generated through direct or complex deletion of the interstitial region (referred to as "deletion"), and the others are formed through insertional chromosomal rearrangements that maintain the interstitial region (referred as to "insertion") (1,2). Both fusion mechanisms result in androgen receptor–driven ERG overexpression.

Despite 17 years of devoted research, the impact of fusion-associated ERG overexpression on clinical outcomes remains controversial (1,3,4). Nevertheless, there is a consensus that the

deletion prostate cancer subtype is more aggressive than the insertion subtype, as it is associated with higher tumor stages, presence of pelvic lymph node metastases, and poorer disease-specific and overall survival (1,2,5). Patients with biallelic deletion-derived fusion had worse survival than those with monoallelic deletion-derived fusion (6). Deletion-derived fusion is detected 3 times more frequently in metastatic castration-resistant prostate cancer than in hormone-naïve cases (5). A study of patients who died of metastatic castration-resistant prostate cancer showed that all metastatic sites harboring TMPRSS2-ERG fusions were of the deletion subtype (7). Conversely, insertion-derived fusion was five- to sixfold more enriched in low-risk prostate cancers than in intermediate- and high-risk prostate cancers (2).

The more aggressive nature of the deletion subtype is also reflected in transgenic models. Prostatic hyperplasia was detected in 19% of the mice with deletion-derived fusion but not in any mice with insertion-derived fusion (8). In the background of biallelic *Pten* loss, approximately 60% of the mice with deletion-derived fusion, but none with insertion-derived fusion, developed poorly differentiated invasive prostate cancers by 12 months (9).

The interstitial region comprises 16 coding and more than 18 noncoding genes. Based on the aggressive phenotype associated with interstitial deletion, we hypothesized that the aggressive phenotype is due to loss of tumor-suppressor genes in this region. Among these interstitial genes, only E26 transformation-specific proto-oncogene 2 (ETS2) has been shown to have tumor-suppressor function in prostate cancer (9,10), although its tumor-promoting activity in prostate cancer has also been implicated (11,12). Here, we undertook an unbiased approach to address the largely ignored, yet crucial role, of interstitial-gene loss in promoting prostate cancer progression and identified FAM3B as a key tumor-suppressor gene in the region.

Methods
Statistical analysis
H-scores were analyzed by Mann–Whitney test. Kaplan–Meier survival curves were compared using log-rank test. Cell and tumor growth was analyzed by linear-regression comparison. Two groups were compared using 2-sided Welch t test. See Supplementary Methods (available online) for others.

Results
Loss of FAM3B and prostate cancer progression
Not all interstitial genes are uniformly lost in the deletion prostate cancer subtype (2). To identify interstitial genes with functional associations with prostate cancer progression, we assessed their expression across the primary and metastatic adenocarcinoma samples with TMPRSS2-ERG fusion in the RNA-sequencing data from The Cancer Genome Atlas program, the Stand Up To Cancer (SU2C) (13), and the Prostate Cancer Medically Optimized Genome-Enhanced Therapy (PROMOTE) cohorts (14) and Grasso microarray dataset (10). BACE2, FAM3B, MX1, PCP4, SH3BGR, and WRB, but not ETS2, were downregulated in metastatic compared with primary adenocarcinomas in 1 or both datasets (Figure 1, A; Supplementary Figure 1, A, available online). Among these genes, FAM3B levels showed the strongest negative correlation with Gleason scores and grade groups in primary prostate cancers (Figure 1, B; Supplementary Figure 1, B-F, available online). Moreover, low FAM3B was associated with faster disease

progression after prostatectomy (Figure 1, C). Notably, the association between FAM3B loss and prostate cancer aggressiveness was also present in fusion-negative prostate cancers (Figure 1, D-F), indicating the existence of interstitial-deletion-unrelated FAM3B-silencing mechanisms.

We then validated the above findings using additional microarray datasets (10,15). Consistently, FAM3B was downregulated when prostate cancer became castration resistant (Supplementary Figure 2, A and B, available online). Moreover, FAM3B expression decreased with higher pathological stage, faster biochemical recurrence, and higher Decipher score, a metastasis-predicting genomic score (16) (Supplementary Figure 2, C-E, available online). Thus, the analysis of microarray datasets validated our findings from the RNA-sequencing datasets.

To determine whether FAM3B protein expression mirrors its RNA expression, we performed immunohistochemistry on tissue microarrays containing 109 hormone-naïve and 19 castration-resistant primary prostate cancer tissue cores after validating FAM3B antibody specificity (Supplementary Figure 3, available online). The hormone-naïve samples exhibited strong apical, dot-like cytoplasmic staining, whereas the castration-resistant samples produced minimal signals (Figure 2, A). Moreover, the hormone-naïve prostate cancers with low FAM3B staining recurred faster and had a higher Gleason score, grade group, and pathological stage than those with high FAM3B staining (Figure 2, B-D). Collectively, the above data support FAM3B as the top-ranked interstitial gene whose loss is associated with disease progression.

Effect of FAM3B on the growth of prostate cancer cells and xenografts
To study the biological significance of the association, we performed colony-formation assays in LNCaP, C4-2, and LNCaP95 cells with or without constitutive or doxycycline-induced FAM3B expression. LNCaP is androgen sensitive, and LNCaP95 and C4-2 are castration-resistant LNCaP derivatives. They are TMPRSS2-ERG negative (17) and express minimal FAM3B. FAM3B inhibited their colony-forming ability (Figure 3, A). Similarly in xenograft models, FAM3B expression inhibited the growth of castration-resistant LuCaP35CR patient-derived xenograft (18), and FAM3B knockdown via different short hairpin RNAs promoted the growth of androgen-sensitive LuCaP136 patient-derived xenograft (19) and castration-resistant progression of VCaP tumors (Figure 3, B-D). The resected VCaP tumors in the knockdown group showed a higher proliferation rate than the control tumors (Figure 3, E). LuCaP35CR and VCaP contain TMPRSS2-ERG fusion, which was caused by deletion in LuCaP35CR and by insertional rearrangement in VCaP (5). LuCaP136 is TMPRSS2-ERG negative (19). Thus, the growth-suppressive function of FAM3B in these models is irrespective of TMPRSS2-ERG fusion.

FAM3B is secreted by the pancreas and liver and regulates glycemic levels via a paracrine or endocrine manner (20,21). Likewise, we detected FAM3B protein in the conditioned medium from FAM3B-expressing C4-2 cells and in the extracellular space of FAM3B-expressing C4-2 xenografts (Supplementary Figure 4, A and B, available online). Additionally, a large fraction of intracellular FAM3B was localized to the endoplasmic reticulum and Golgi, typical of secretory proteins, although a notable localization to the rest of the cytoplasm was also observed (Supplementary Figure 4, C, available online). However, unlike intracellular FAM3B expression, treating prostate cancer cells with FAM3B-containing conditioned medium did not alter their colony-forming ability (Supplementary Figure 4, D, available
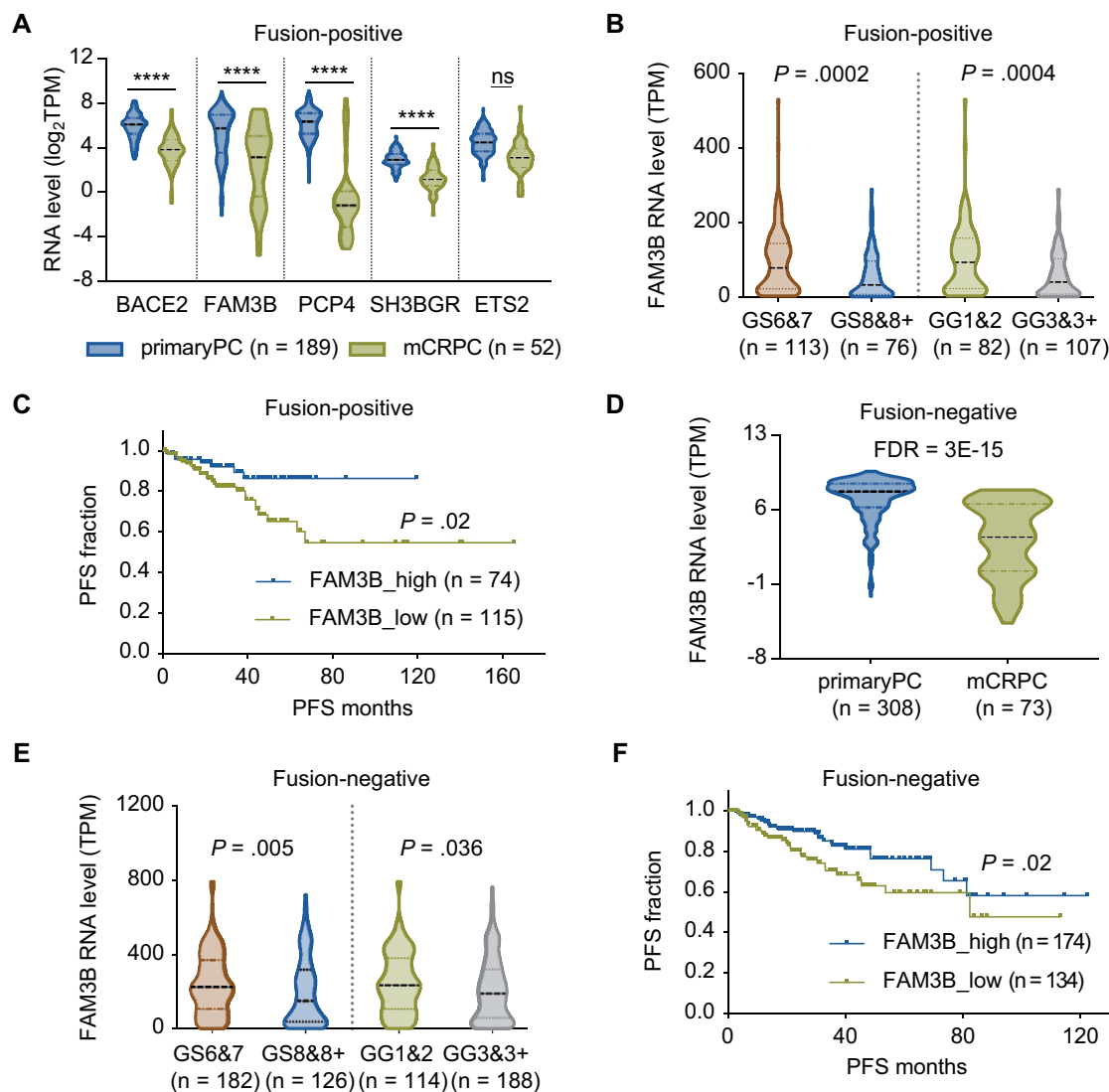
Figure 1. Loss of FAM3B RNA expression and prostate cancer prognosis. **A)** Four interstitial genes are downregulated in fusion-positive metastatic castration-resistant prostate cancer compared with primary prostate cancers. Metastatic castration-resistant prostate cancers were from the Stand Up To Cancer (SU2C) and the Prostate Cancer Medically Optimized Genome-Enhanced Therapy (PROMOTE) cohorts, and primary prostate cancers were from The Cancer Genome Atlas (TCGA) cohort. Genes that are expressed at very low levels (mean transcript per million (TPM) < 5 in both groups) are excluded from the analysis. **** False discovery rate (FDR) < .0001 and |fold of change (FC)| > 1.5 by Differential gene expression analysis based on the negative binomial distribution (DEseq). **B-F)** In both fusion-positive **(B, C)** and -negative **(E, F)** TCGA primary prostate cancers, low FAM3B RNA levels are associated with high Gleason scores and grade groups and a short time to disease progression. **D)** FAM3B RNA is downregulated in fusion-negative metastatic castration-resistant prostate cancer compared with primary prostate cancers. FDR from DEseq. P values from Mann–Whitney **(B, E)** or log-rank test **(C, F)**. **C, F)** High and low groups are separated based on the median value of the expression. GG = grade group; GS = Gleason score; mCRPC = metastatic castration-resistant prostate cancer; PC = prostate cancer; PFS = progression-free survival.

online), suggesting that FAM3B growth inhibition in prostate cancer is likely mediated through intracellular, rather than extracellular, mechanisms.

Effect of FAM3B loss on prostate cancer progression in Hi-Myc mice

We then used a conventional FAM3B-knockout mouse model (22) to further verify the growth-suppressive function of FAM3B. In the wild-type mice, FAM3B was highly expressed in prostate luminal epithelial cells and in the pancreas and kidney (Supplementary Figure 5, A and B, available online). Notably, $Fam3b^{-/-}$ and $Fam3b^{+/+}$ mice displayed comparable prostate-gland architecture and epithelial proliferation rate up to 12 months (Supplementary Figure 5, C and D, available online),

indicating that FAM3B loss alone is insufficient to initiate prostate tumorigenesis.

To further assess the impact of FAM3B knockout on prostate cancer progression, we crossed $Fam3b^{-/-}$ mice with Hi-Myc mice, which express high Myc levels specifically in the prostate and recapitulate the spectrum of lesions in human prostate cancer (23). Because the 2 mouse models have different genetic backgrounds, we backcrossed $Fam3b^{+/-}$/Hi-Myc mice to Hi-Myc mice for more than 5 generations to eliminate genetic differences as a confounding factor. At 5 months, although the genitourinary-bloc morphology and weight were comparable between $Hi-Myc/Fam3b^{-/-}$ and $Hi-Myc/Fam3b^{+/+}$ mice (Figure 4, A), FAM3B loss led to more invasive adenocarcinoma, faster epithelial proliferation, greater angiogenesis, and less apoptosis in the prostate (Figure 4,
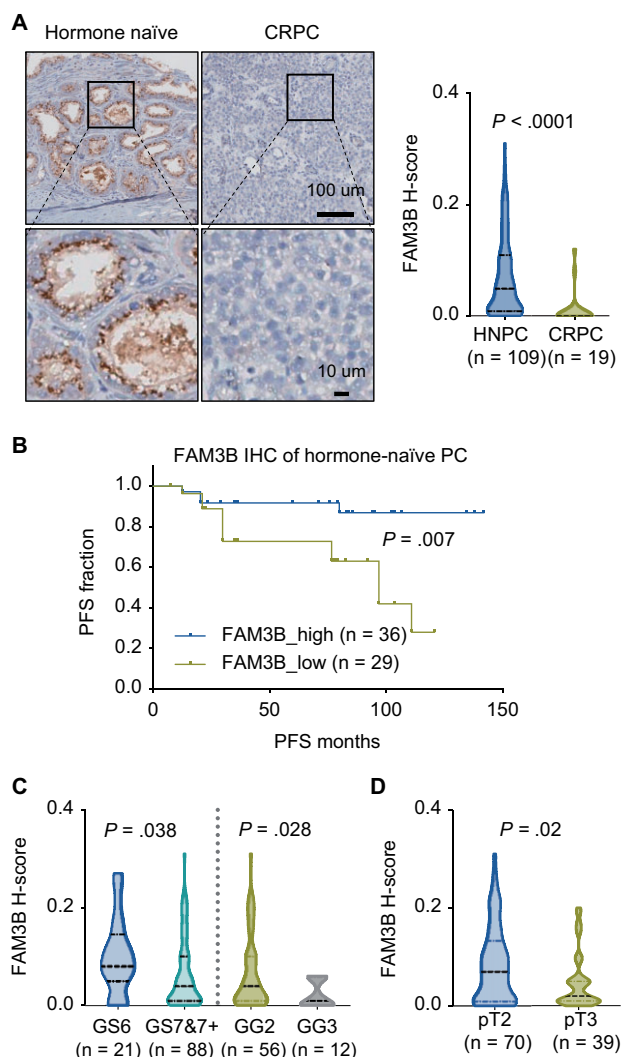
Figure 2. Loss of FAM3B protein expression and prostate cancer progression. FAM3B immunohistochemistry of tissue microarrays shows loss of FAM3B protein in castration-resistant compared with hormone-naïve primary prostate cancers **(A)** and association of low FAM3B protein level with a short time to disease progression **(B)**, high Gleason score **(C)**, grade group **(C)**, and pathological stage (pT) **(D)** in hormone-naïve prostate cancer. P values from Mann–Whitney **(A, C, D)** or log-rank test **(B)**. High and low groups in **panel C** are separated based on the median value of the expression. pT2 includes pT2, pT2a, pT2b, and pT2c; and pT3 includes pT3a and pT3b. CRPC = castration-resistant prostate cancer; GG = grade group; GS = Gleason score; IHC = immunohistochemistry; PC = prostate cancer; PFS = progression-free survival.

B-E), supporting the role of FAM3B loss in driving prostate cancer progression.

Contribution of androgen deprivation to FAM3B loss

The association between FAM3B loss and prostate cancer aggressiveness in fusion-negative prostate cancer (Figure 1, D-F) suggests the existence of fusion-unrelated FAM3B-silencing mechanisms and the potential significance of these mechanisms in prostate cancer outcome. Based on FAM3B downregulation when primary prostate cancers (Figure 2, A; Supplementary Figure 2, A and B, available online) and VCaP tumors (Figure 5, A) became castration resistant, we asked whether androgen-deprivation therapy silences FAM3B expression. Comparing RNA-sequencing data from matched pre- and postandrogen-
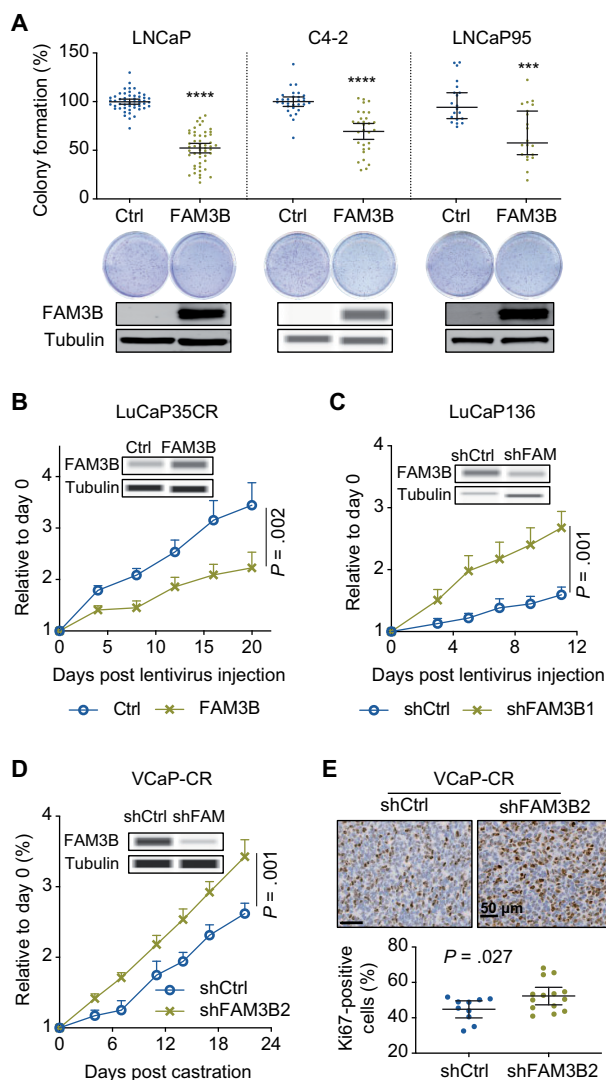
Figure 3. Effect of FAM3B on prostate cell growth and castration-resistant progression. **A)** FAM3B expression in LNCaP (constitutive), C4-2 (induced), and LNCaP95 (constitutive) cells inhibits their colony formation in soft agar. **Bottom panel,** Western blotting. **B and C)** FAM3B expression inhibits the growth of LuCaP35CR patient-derived xenograft **(B)**, and FAM3B knockdown induces the growth of LuCaP136 patient-derived xenograft **(C)**. FAM3B expression or knockdown was achieved via intratumoral injection of lentivirus expressing FAM3B or FAM3B short hairpin RNA (shRNA)-1 (shFAM3B1). **Insets**, capillary Western blotting; $n = 6$ for the control (Ctrl) and control shRNA (shCtrl) groups; $n = 7$ for the FAM3B and shFAM3B (shFAM) groups. **D and E)** FAM3B knockdown promotes castration-resistant progression of VCaP xenograft tumor **(D)** and Ki67 proliferation indices of the tumors **(E)**. FAM3B knockdown was achieved via transduction of cells with lentivirus expressing FAM3B shRNA-2 (shFAM3B2). Mice were castrated when tumors reached 100 mm³; $n = 10$ for the shCtrl group; $n = 14$ for the shFAM3B2 group. *** $P < .0005$; **** $P < .0001$; P values in **panels A and E** from Welch t test. P values in other panels from comparison via linear regression. Ctrl = control; PC = prostate cancer; PDX = patient-derived xenograft.

deprivation therapy prostate cancer specimens (24), we found reduced FAM3B expression after androgen-deprivation therapy (Figure 5B). Similarly, castration decreased FAM3B expression in mouse prostate (Figure 5, C). Conversely, treating VCaP cells with the R1881 synthetic androgen (25) or dihydrotestosterone (DHT) led to FAM3B induction, which was blocked by enzalutamide, an androgen receptor antagonist, although the induction was associated with initial transient repression (Figure 5, D-G). Rapid
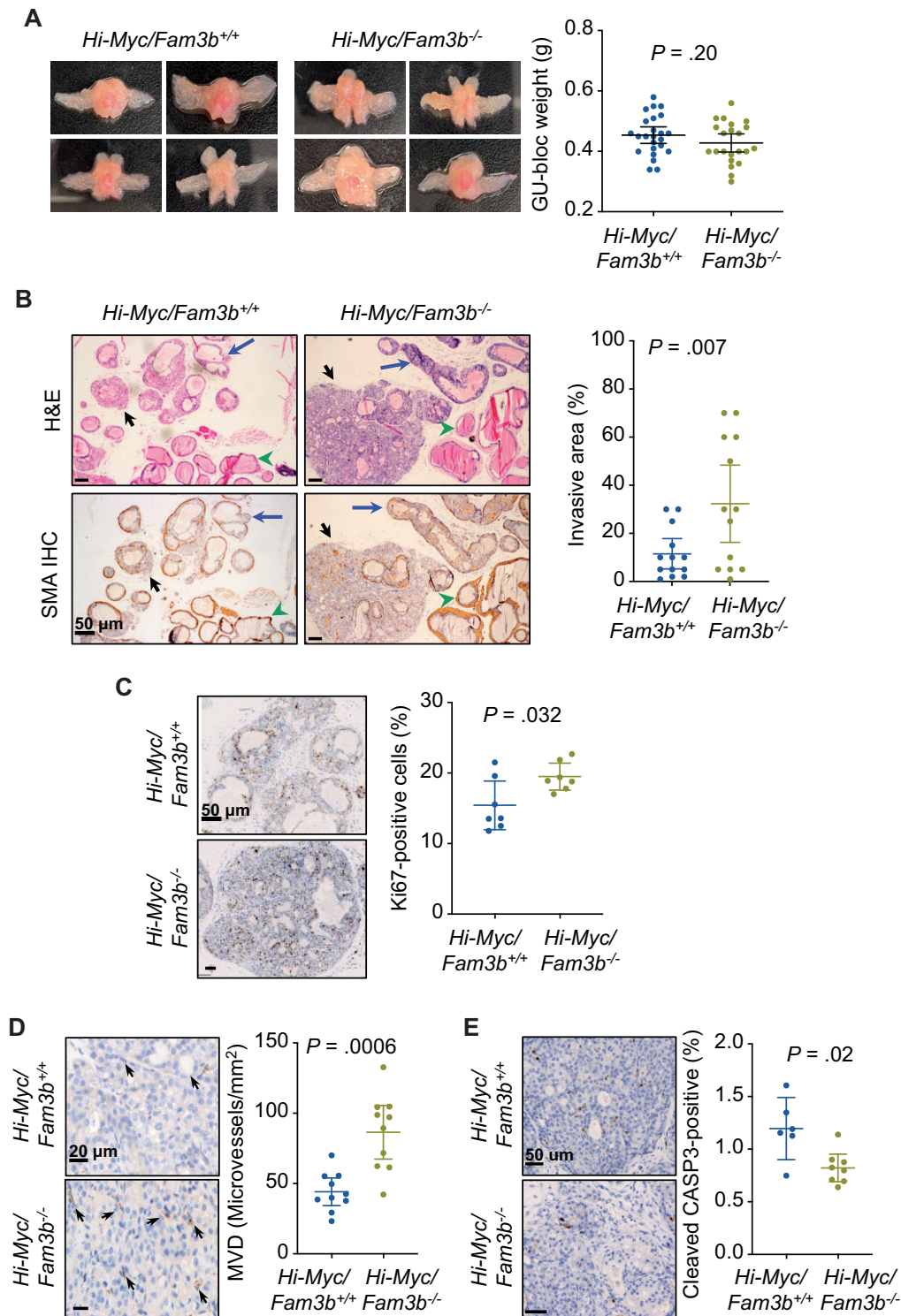
Figure 4. Effect of FAM3B knockout on prostate cancer progression in Hi-Myc mice. **A)** *Hi-Myc/Fam3b⁻/⁻* mice display no statistically significant change in genitourinary (GU)-bloc morphology or weight from *Hi-Myc/Fam3b⁺/⁺* mice at 5 months of age. **B)** FAM3B knockout leads to more invasive prostate adenocarcinoma in Hi-Myc mice at 5 months of age. **Arrowheads**, benign glands; **long arrows**, high-grade prostatic intraepithelial neoplasia (PIN); **short arrows**, invasive adenocarcinoma. **C-E)** The dorsal lateral prostates in *Hi-Myc/Fam3b⁻/⁻* mice have increased epithelial Ki67 proliferation index **(C)** and microvessel density **(D)** and decreased levels of cleaved caspase-3 **(E)** than those in *Hi-Myc/Fam3b⁺/⁺* mice. **Arrows** in **panel D**, microvessels. *P* values from Welch *t* test. H&E = hematoxylin and eosin; IHC = immunohistochemistry; SMA = smooth-muscle actin; MVD = microvessel density.

alternations between high-dose androgen and androgen-deprivation therapy, the bipolar androgen therapy, have shown promise in resensitizing metastatic castration-resistant prostate cancer to androgen receptor–signaling inhibitors (26). We found that feeding VCaP cells with supraphysiological-level androgen (Figure 5, H and I) after androgen deprivation produced a similar pattern of FAM3B modulation as physiological-level androgens (Figure 5, D-G). These results support androgen deprivation as a
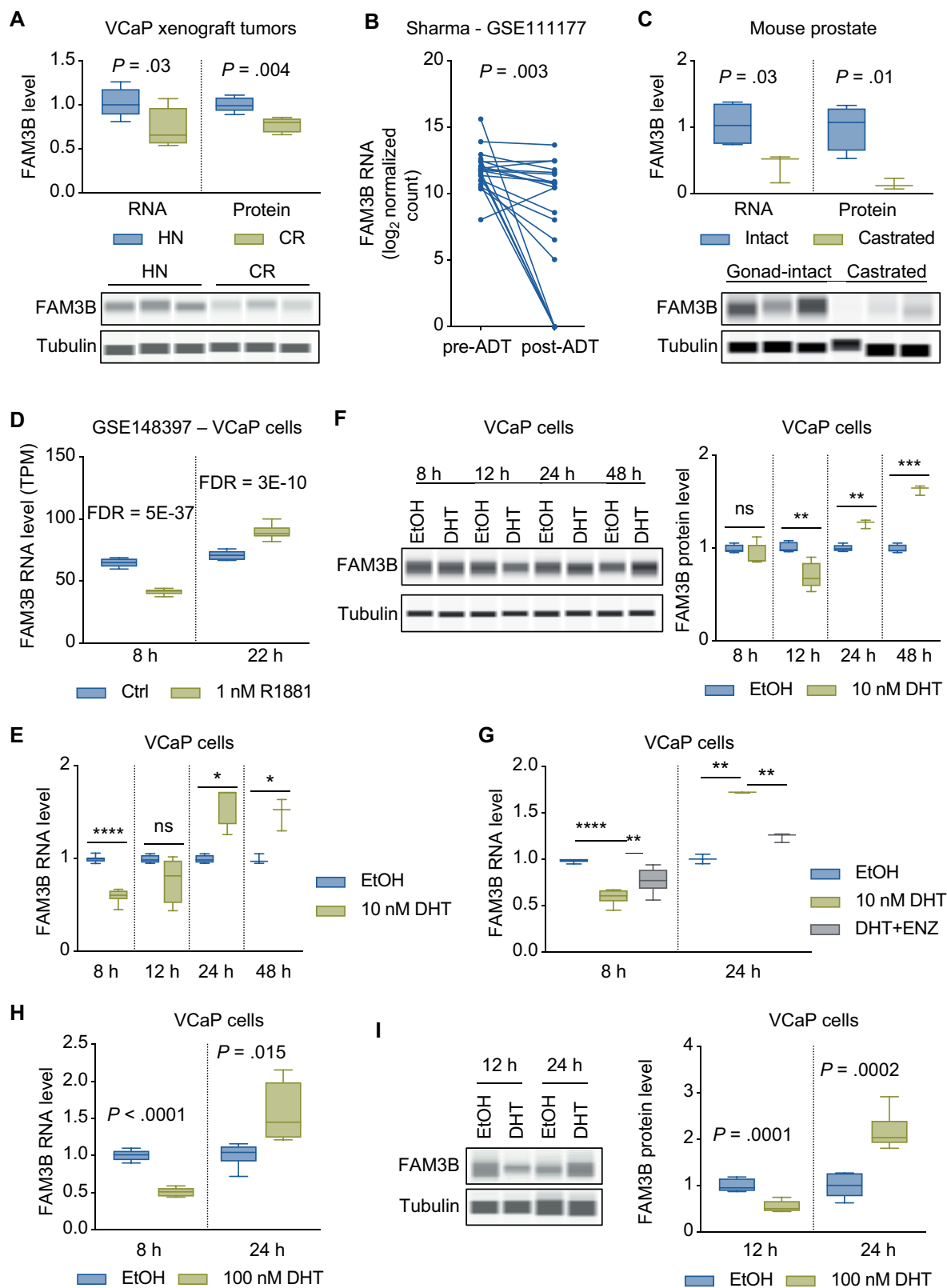
Figure 5. Effect of androgen deprivation on FAM3B expression. **A)** FAM3B RNA and protein levels are reduced in castration-resistant VCaP tumors compared with the hormone-naïve counterpart; n = 6-8. **B)** FAM3B RNA levels are reduced in prostatectomy samples post–androgen-deprivation therapy (1-8 months; median 3 months). **C)** Castration causes decreased expression of FAM3B RNA and protein in the prostate in 4-month-old C57BL/6 mice. Tissues were collected 2 days after castration; n = 3 or 4. **D-I)** In response to androgen treatment, FAM3B RNA **(D, E, G, H)** and protein **(F, I)** are upregulated in VCaP cells, following a transient downregulation. RNA levels in **panels B** and **D** were from RNA-sequencing, and those in other panels were from real-time quantitative PCR. **Bottom panel A, C; left panel F, I)** Capillary Western blots. EtOH = ethanol; DHT = dihydrotestosterone; ENZ = 20 uM enzalutamide. *P* value in **panel B** from paired *t* test. *P* values in other panels from Welch *t* test. False discovery rate from DEseq. *P < .05. **P < .005. ***P < .0005. ****P < .0001. ADT = androgen-deprivation therapy; CR = castration-resistant; FDR = false discovery rate; HN = hormone-naïve; ns = not significant.
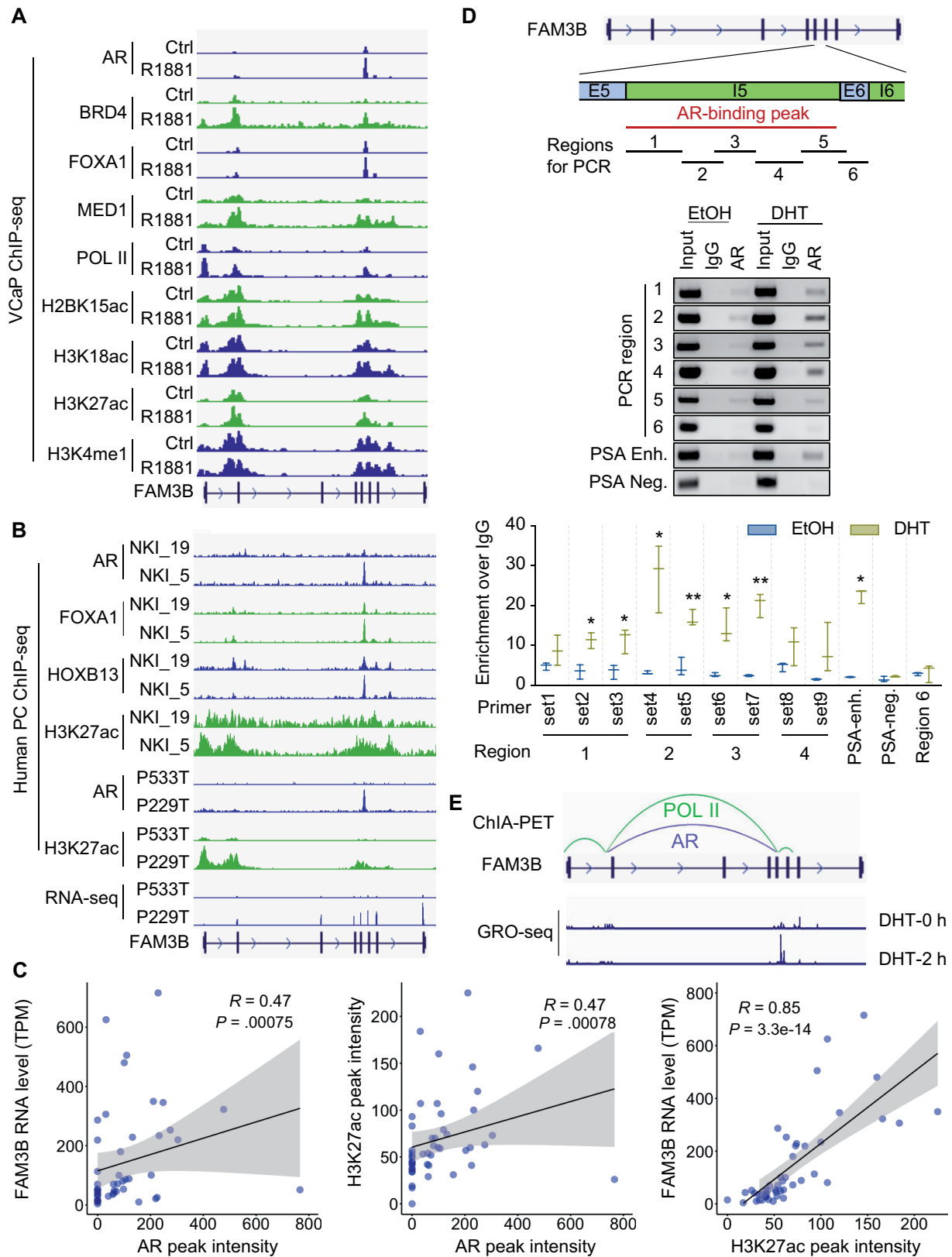
Figure 6. Androgen receptor regulation of FAM3B transcription. **A)** ChIP-sequencing data from VCaP cells (GSE148358) show that androgen receptor co-occupies FAM3B intron-5 with other transcription factors, RNA polymerase II, and active histone marks and that the co-occupancy is enhanced by androgen. R1881 = 1 nM for 22 h. **B, C)** ChIP-sequencing and RNA-sequencing data from human prostate cancer samples show that androgen receptor co-occupies FAM3B intron-5 with other transcription factors and the H3K27ac active histone mark in clinical samples **(B)** and that the intensity of androgen receptor binding positively correlates with the level of FAM3B RNA and the intensity of H3K27ac binding **(C)**. Samples NKI_19 and NKI_5 are

fusion-independent FAM3B-silencing mechanism and the potential to restore FAM3B expression by bipolar androgen therapy.

Androgen receptor binding to FAM3B intron-5

Because androgen regulation occurs initially at FAM3B RNA level, we asked whether FAM3B is an androgen receptor transcriptional target. Using publicly available chromatin immunoprecipitation (ChIP)–sequencing datasets from VCaP cells (25) and primary prostate cancers (27,28), we discovered that androgen receptor co-occupies FAM3B intron-5 with other transcription factors, RNA polymerase II, and active histone marks (29-31) (Figure 6, A and B). Importantly, there was a high concordance between the binding intensities of these trans-acting factors and that of androgen receptor and between androgen receptor binding and FAM3B RNA levels (Figure 6, B and C). Using the ChromHMM chromatin-state characterization pipeline (32), we classified FAM3B intron-5 as an enhancer (Supplementary Figures 6, A and 7, A, available online). FAM3B levels in different normal tissues correlated with the presence or absence of this enhancer activity (Supplementary Figure 6, B, available online). To confirm androgen receptor binding, we divided the approximate 1.3 kb intron-5 into 5 regions, and ChIP–PCR showed androgen-induced androgen receptor binding to regions 1 to 4 and the positive-control prostate-specific antigen (PSA)–enhancer region, but not region-5, the flanking region-6, or a nonandrogen receptor–binding PSA locus (Figure 6, D). ChIP–quantitative PCR further confirmed androgen-induced androgen receptor binding to regions 1 to 3, a 675 bp sequence (Figure 6, D).

In addition to stimulating the binding of androgen receptor and other factors to intron-5, androgen caused an overall enhanced association of these factors (except androgen receptor) with a FAM3B intron-1 locus and/or the proximal promoter (Figure 6, A), suggesting that androgen receptor may regulate FAM3B transcription through chromatin looping, a common mode of androgen receptor regulation (33). Supporting this notion, we detected androgen receptor- and RNA polymerase II–chromatin interactions spanning the promoter, the intron-1 locus, and intron-5 enhancer in VCaP Chromatin Interaction Analysis with Paired-End-Tag sequencing (ChIA-PET) data (34,35) (Figure 6, E). Moreover, Global run-on (GRO) sequencing (35) revealed androgen-induced production of a noncoding RNA predominantly from the opposite strand of the intron-5 enhancer (ie, an antisense enhancer RNA) (Figure 6, E). Although enhancer RNAs promote enhancer-promoter looping at certain loci to enhance transcription (36), transcription at intragenic enhancers, especially antisense transcription, can cause a pause of the host mRNA transcription to fine-tune host-gene transcription (37). This may underlie the initial transient FAM3B decline in response to androgen (Figure 5, D-I). A similar pattern of androgen regulation was displayed by other genes with an androgen receptor–binding intragenic enhancer(s) (Supplementary Figure 7, B-D, available online).

Collectively, the above results identified FAM3B as a direct androgen receptor target. Liganded androgen receptor binds to a FAM3B intron-5 enhancer to stimulate enhancer RNA expression and facilitate enhancer-promoter looping to activate FAM3B transcription. Through this mechanism, intact androgen receptor signaling facilitates FAM3B expression, whereas androgen deprivation enables fusion-independent FAM3B silencing.

Contribution of promoter hypermethylation to FAM3B silencing

Without androgen-deprivation therapy or fusion-associated deletion, hormone-naïve prostate cancers can still lose FAM3B expression as they progress (Figure 1, E and F), indicating the existence of additional FAM3B-silencing mechanisms. The FAM3B promoter contains a robust CpG island, and 8 CpG sites around this island were methylated in the The Cancer Genome Atlas prostate cancer samples (Figure 7, A). Importantly, there is a strong negative correlation between the methylation levels of each of these CpG sites and FAM3B levels (Figure 7, A). Moreover, hypermethylation of 5 of these CpG sites was associated with fast disease progression in fusion-negative and/or -positive prostate cancers (Figure 7, B; Supplementary Figure 8, A and B, available online). Because the cg18440523 site was associated with disease progression in both populations (Figure 7, B), we performed bisulfite-amplicon sequencing with this site for validation. Treatment of VCaP and C4-2 cells with the decitabine DNA-methyltransferase inhibitor decreased cytosine methylation and increased FAM3B expression (Figure 7, C-E). Furthermore, decitabine inhibited the colony-forming ability and growth of these cells (Figure 7, F and G; Supplementary Figure 8, C, available online), and FAM3B knockdown attenuated decitabine growth suppression (Supplementary Figure 8, D, available online). These data indicate that promoter hypermethylation is an additional FAM3B-silencing mechanism in advanced prostate cancer. We found that these 2 epigenetic imprinting mechanisms may not intersect as androgen deprivation did not alter the level of FAM3B promoter methylation (Supplementary Figure 8, E and F, available online).

FAM3B modulating androgen receptor transcriptional activity

To understand how FAM3B loss promotes prostate cancer progression, we performed RNA sequencing of castration-resistant VCaP tumors with or without FAM3B knockdown and C4-2 cells with or without doxycycline-induced FAM3B expression. Gene set enrichment analysis identified 12 pathways enriched after FAM3B

Figure 6. Continued

from the GSE130408 dataset, and samples P533T and P229T as well as the correlation data presented in **panel C** are from the GSE120738 dataset. R and P values are from Spearman correlation analysis. **D)** ChIP-PCR and ChIP-quantitative-PCR confirmation of androgen receptor binding to FAM3B intron-5. **Top panel**, a schematic diagram showing the subregions of FAM3B introns-5 and -6 that were PCR amplified in ChIP-PCR. **Middle panel**, ChIP-PCR results with immunoglobulin G or the androgen receptor N-20 antibody. **Bottom panel**, ChIP-quantitative-PCR results with multiple sets of primers covering regions 1-4 of FAM3B intron-5. Dihydrotestosterone = 10 nM for 4 h. Prostate-specific antigen (PSA) enhancer = androgen receptor-binding PSA enhancer region as a positive control. PSA negative = nonandrogen receptor-binding PSA locus as a negative control. *P < .05; **P < .005 from the EtOH group using Welch t test. **E)** Chromatin Interaction Analysis with Paired-End-Tag sequencing (ChIA-PET) and Global run-on sequencing (GRO-seq) data from VCaP cells (GSE54946 and GSE121020) show androgen receptor- and RNA polymerase II-associated chromatin looping and androgen-induced expression of an enhancer RNA from androgen receptor-binding FAM3B intron-5. AR = androgen receptor; ChIP = chromatin immunoprecipitation; Ctrl = control; EtOH = ethanol; DHT = dihydrotestosterone; Enh = enhancer; IgG = immunoglobulin G; Neg = negative; PC = prostate cancer; POL II = RNA polymerase II; TPM = transcript per million.
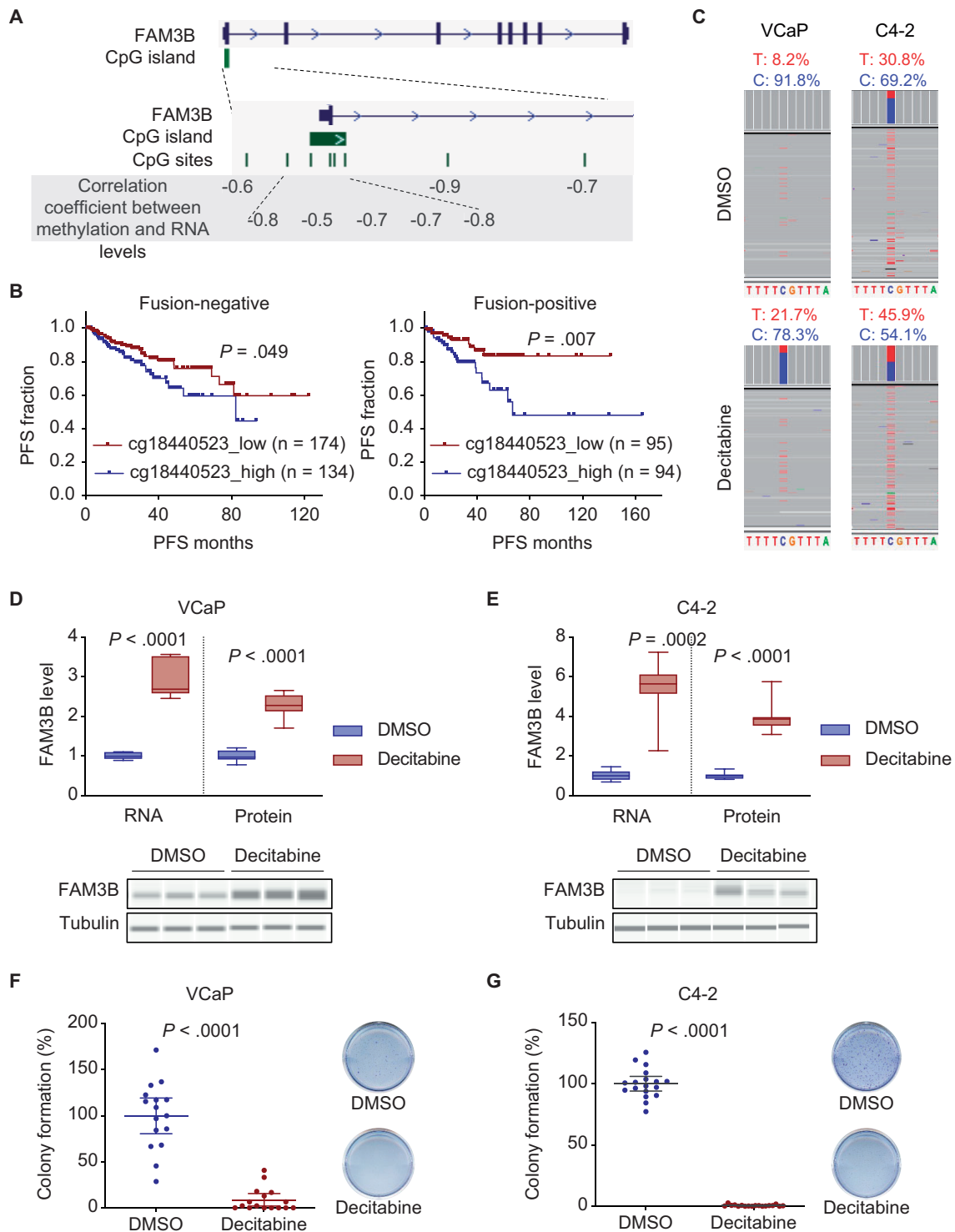
Figure 7. FAM3B promoter hypermethylation. **A)** FAM3B promoter contains a CpG island, and its methylation levels correlate negatively with FAM3B expression in The Cancer Genome Atlas (TCGA) prostate cancers. **Top**, FAM3B CpG island (**green bar**) on the University of California Santa Cruz (UCSC) genome browser. **Middle**, CpG island and 5' end of FAM3B in higher magnification. **Bottom**, methylated CpG sites from TCGA prostate cancer methylation array data and the Spearman correlation coefficients between the methylation levels of each CpG site and FAM3B mRNA levels in TCGA prostate cancers (n = 497). **B.** In both fusion-negative and -positive TCGA prostate cancers, high methylation of the cg18440523 CpG site is associated with fast disease progression. High and low groups are separated based on the median methylation level. **C)** Bisulfite amplicon sequencing shows that decitabine treatment of VCaP and C4-2 cells decreases cytosine methylation in cg18440523 (methylated cytosine remains intact after bisulfite conversion). **D, E)** Decitabine treatment increases FAM3B expression in VCaP **(D)** and C4-2 cells **(E)**. RNA and protein were assessed by real-time quantitative PCR capillary Western analysis, respectively. **F, G)** Decitabine treatment inhibits the colony-forming ability of VCaP **(F)** and C4-2 cells **(G)**. Decitabine = 1 uM. P values in **panel B** from log-rank test. P values in other panels from Welch t test. AR = androgen receptor; PC = prostate cancer; PFS = progression-free survival; DMSO = dimethyl sulfoxide; T = thymine; C = cytosine.
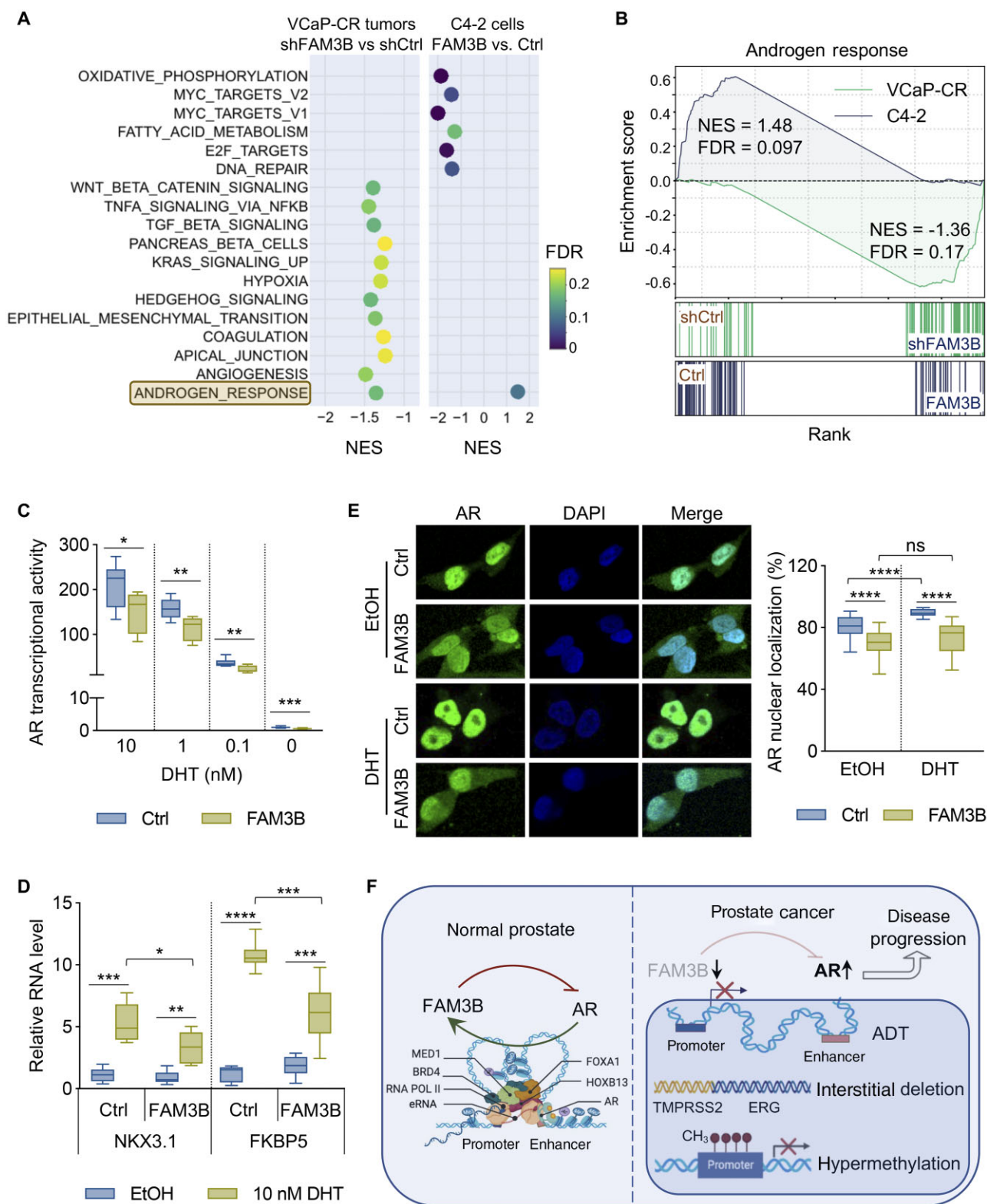
Figure 8. FAM3B regulation of androgen receptor transcriptional activity. **A)** Gene set enrichment analysis of RNA-sequencing data from VCaP castration-resistant tumors with or without FAM3B knockdown and C4-2 cells with or without doxycycline-induced FAM3B expression identifies the androgen-response pathway as the only overlapping pathway modulated by FAM3B in the 2 models. **B)** Gene set enrichment analysis plots of the androgen-response pathway in the 2 models. **C, D)** Luciferase assay with the ARR3-luc construct **(C)** and real-time quantitative PCR analyses of androgen receptor targets **(D)** in doxycycline-inducible FAM3B-expressing C4-2 cells confirm FAM3B inhibition of androgen receptor transcriptional activity. **E)** Androgen receptor immunofluorescent staining of doxycycline-inducible FAM3B-expressing C4-2 cells cultured in androgen-depleted condition treated with 10 nM dihydrotestosterone or vehicle control shows FAM3B attenuation of androgen receptor nuclear localization. The percent of androgen receptor nuclear localization was calculated based on the fraction of nuclear androgen receptor fluorescence intensity in each cell. **F)** Model of androgen receptor and FAM3B feedback regulation in normal prostate or prostate cancer. $*P < .05$; $**P < .005$; $***P < .0005$; $****P < .0001$; ns = not significant using Welch t test. AR = androgen receptor; Ctrl = control; CR = castration resistant; EtOH = ethanol; DHT = dihydrotestosterone; FDR = false discovery rate; GSEA = gene set enrichment analysis; NES = normalized enrichment score.

knowledge in VCaP tumors and 7 pathways enriched after FAM3B expression in C4-2 cells (Figure 8, A). Interestingly, the androgen-response pathway was the only overlapping pathway. Gene set enrichment analysis plots (Figure 8, B) and androgen receptor–activity scores (Supplementary Figure 9, A, available online) indicated high androgen-response signaling in the FAM3B-low groups, suggesting FAM3B inhibition of androgen receptor signaling.

Consistently, FAM3B expression inhibited the activity of an androgen receptor–responsive luciferase reporter and androgen-induced androgen receptor–target expression (Figure 8, C and D; Supplementary Figure 9, B, available online). These experiments were concluded before alteration in cell growth to ensure that the changes were not secondary to growth inhibition. We also assessed androgen receptor–target expression after treating C4-2 cells with a FAM3B-containing conditioned medium or a recombinant FAM3B protein (38). Consistent with the colony-formation data (Supplementary Figure 4, D, available online), the extracellular FAM3B protein did not statistically significantly impact androgen receptor–target expression (Supplementary Figure 9, C and D, available online). These data support the role of FAM3B in inhibiting androgen receptor transcriptional activity through intracellular mechanisms.

To address the underlying mechanism, we assessed androgen receptor expression and localization and androgen receptor–FAM3B physical interaction in C4-2 cells. FAM3B did not alter androgen receptor protein level nor was co-immunoprecipitated with androgen receptor (Supplementary Figure 9, E and F, available online). Nevertheless, it caused a 15%-18% decrease in androgen receptor nuclear localization in both androgen-depleted and androgen-repleted conditions (Figure 8, E; Supplementary Figure 9G, available online). Because the impact of FAM3B on androgen receptor nuclear localization is not as pronounced as that on androgen receptor transcriptional activity (>50%; Figure 8, C and D; Supplementary Figure 9, A and B, available online), additional mechanisms, such as androgen receptor posttranslational modification, are likely to be involved. Capitalizing on the androgen receptor–knockout CWR22Rv1-AR-EK cells that retain androgen receptor splicing variants (39), we studied the impact of FAM3B on androgen receptor splicing variants, which have been linked to prostate cancer therapy resistance (40). FAM3B similarly inhibited androgen receptor splicing variant transcriptional activity and nuclear localization without affecting androgen receptor splicing variant expression (Supplementary Figure 10, A-C, available online). Moreover, FAM3B diminished the colony-forming ability of CWR22Rv1-AR-EK cells without affecting the colony-forming ability or growth of the androgen receptor–null DU145 and PC-3 cells (Supplementary Figure 10, D-G, available online). Because FAM3B was shown by a previous study to promote DU145 growth under a serum-starved condition (41), we reassessed the impact of FAM3B on DU145 and PC-3 cells under the same serum-starved condition by 3-[4,5-dimethylthiazol-2-yl]-2,5 diphenyl tetrazolium bromide (MTT) assay, the method used in their study (41). Still, these cells were unresponsive to FAM3B modulation (Supplementary Figure 10, H and I, available online). A possible explanation for the discrepancy might be divergence of DU145 cells in different labs. Together, our findings suggest that FAM3B growth suppression is limited to androgen receptor–positive cells and tumors through its intracellular activity that attenuates androgen receptor signaling. Although FAM3B may support growth suppression through multiple mechanisms, with the androgen receptor pathway being the only overlapping pathway in VCaP and C4-2 (Figure 8, A) and the known importance of androgen receptor activity in prostate cancer

growth and progression, FAM3B suppression of androgen receptor activity is likely a key contributor.

Discussion

We identified a new functional ramification of the TMPRSS2-ERG fusion—loss of FAM3B, a novel tumor suppressor, in driving prostate cancer progression. Our unbiased analysis of the interstitial genes across transcriptome data of large collections of prostate cancer samples nominated FAM3B as the top-ranked interstitial gene whose loss is associated with poor prognosis. Notably, the association is similarly present in fusion-positive and fusion-negative prostate cancers, supporting a broad impact of FAM3B loss on clinical outcomes and the existence of fusion-unrelated FAM3B-silencing mechanisms. Using cultured cells, patient- and cell line–derived xenograft models in gonad-intact or castrated host, and genetically engineered mouse models, we defined a driver role of FAM3B loss in prostate cancer progression. Ectopic FAM3B expression, whether constitutive or induced, inhibits the colony-forming ability of prostate cancer cells and the growth of patient-derived xenograft. Conversely, FAM3B knockdown induces the growth and castration-resistant progression of patient- or cell line–derived xenograft tumors. Furthermore, FAM3B knockout leads to more invasive prostate adenocarcinoma in Hi-Myc mice. Because these models differ in TMPRSS2-ERG genetics, from no fusion to insertion-derived fusion and deletion-derived fusion, the impact of FAM3B loss on prostate cancer progression is likely TMPRSS2-ERG independent, resonating with the link between FAM3B loss and poor clinical outcomes regardless of TMPRSS2-ERG status.

We discovered promoter hypermethylation and androgen deprivation as 2 fusion-unrelated FAM3B-silencing mechanisms in advanced prostate cancer. Liganded androgen receptor binds to an enhancer in FAM3B intron-5 to stimulate enhancer RNA expression and facilitate enhancer-promoter looping to activate FAM3B transcription. Consequently, androgen deprivation, by preventing androgen receptor from binding to the enhancer, suppresses FAM3B expression. FAM3B imposes a feedback inhibition on androgen receptor signaling. In normal prostate, this feedback loop likely acts as a rheostat to keep androgen receptor activity in check; however, in prostate cancer, loss of FAM3B, due to TMPRSS2-ERG interstitial deletion, FAM3B promoter hypermethylation, and/or androgen deprivation, unleashes androgen-dependent or -independent androgen receptor activity to push disease progression (Figure 8, F).

Because metastatic prostate cancer remains a fatal disease, there is a critical need to identify prostate cancers that will progress to metastatic disease so they can be treated early to stop disease progression. The role of FAM3B loss in driving prostate cancer progression and strong correlations for low FAM3B expression with metastasis, castration resistance, and high risk support the utility of FAM3B loss as a biomarker to better define aggressive tumors. As a functional consequence of deletion-derived TMPRSS2-ERG fusion, FAM3B loss may improve the prognostic value of TMPRSS2-ERG fusion, which has been a subject of controversy for the past 17 years.

Another clinical implication of our study is the potential to restore FAM3B expression through epigenetic means even in prostate cancers with deletion-derived fusion because the fusion is often monoallelic. Decitabine may potentiate enzalutamide efficacy by alleviating enzalutamide-mediated FAM3B downregulation along with restoring the expression of other tumor-suppressor genes. Moreover, our data with supraphysiological-level androgen

support the potential to mitigate androgen-deprivation therapy–caused FAM3B downregulation by alternating androgen-deprivation therapy with high-dose androgen in bipolar androgen therapy (26).

In closing, we unraveled a new functional consequence of TMPRSS2-ERG fusion—loss of FAM3B, a novel tumor suppressor, in driving prostate cancer progression. Our work highlights the utility of FAM3B loss as a biomarker to better define aggressive prostate cancer and improve the prognostic value of TMPRSS2-ERG fusion.

Data availability

All RNA-sequencing data generated in this study have been deposited in the Gene Expression Omnibus with the accession number GSE210202.

Author contributions

Tianfang Ma, PhD (Conceptualization; Data curation; Formal analysis; Methodology; Validation; Visualization; Writing—original draft), Erik K. Flemington, PhD (Funding acquisition; Methodology; Resources; Writing—review & editing), Zongbing You, MD, PhD (Methodology; Writing—review & editing), Jia Fan, PhD (Funding acquisition; Methodology; Resources; Writing—review & editing), Brant R. Burkhardt, PhD (Resources), Lovisa Holmberg Schiavone, PhD (Methodology; Resources; Writing—review & editing), Kun Zhang, PhD (Funding acquisition; Methodology; Writing—review & editing), Melody Baddoo, MS (Methodology), Nathan Ungerleider, PhD (Methodology), Gavisha Mugon, BS (Data curation), Derek Y. Zhang (Formal analysis), Chiyaro Wedderburn, BS (Formal analysis) David Zhang (Formal analysis; Methodology; Writing—review & editing), Ladan Fazli, MD (Formal analysis; Methodology), Meijuan J. S. Sun, PhD (Methodology), Subing Cao, PhD (Formal analysis), Yeyoung Cho, BS (Data curation; Formal analysis; Methodology), Beibei Shen, BS (Formal analysis; Investigation), Shuo Wang, MD (Data curation), Zhan Liu, PhD (Formal analysis; Investigation; Methodology), Shanshan Bai, PhD (Conceptualization; Data curation; Formal analysis; Methodology), Lianjin Jin, PhD (Conceptualization; Data curation; Formal analysis; Methodology; Validation; Writing—review & editing), Xuesen Dong, MD, PhD (Formal analysis; Funding acquisition; Methodology; Resources; Writing—review & editing), and Yan Dong, PhD (Conceptualization; Formal analysis; Funding acquisition; Investigation; Project administration; Resources; Supervision; Writing—original draft; Writing—review & editing).

Funding

Conflicts of interest

The authors declare no potential conflicts of interest.

Acknowledgements

References

1. Tomlins SA, Bjartell A, Chinnaiyan AM, et al. ETS gene fusions in prostate cancer: from discovery to daily clinical practice. *Eur Urol*. 2009;56(2):275-286.

2. Murphy SJ, Kosari F, Karnes RJ, et al. Retention of interstitial genes between TMPRSS2 and ERG is associated with low-risk prostate cancer. *Cancer Res*. 2017;77(22):6157-6167.

3. Bostrom PJ, Bjartell AS, Catto JW, et al. Genomic predictors of outcome in prostate cancer. *Eur Urol*. 2015;68(6):1033-1044.

4. Gasi Tandefelt D, Boormans J, Hermans K, et al. ETS fusion genes in prostate cancer. *Endocr Relat Cancer*. 2014;21(3): R143-52.

5. Perner S, Demichelis F, Beroukhim R, et al. TMPRSS2:ERG fusion-associated deletions provide insight into the heterogeneity of prostate cancer. *Cancer Res*. 2006;66(17):8337-8341.

6. Attard G, Clark J, Ambroisine L, et al.; Transatlantic Prostate Group. Duplication of the fusion of TMPRSS2 to ERG sequences identifies fatal human prostate cancer. *Oncogene*. 2008;27 (3):253-263.

7. Mehra R, Tomlins SA, Yu J, et al. Characterization of TMPRSS2-ETS gene aberrations in androgen-independent metastatic prostate cancer. *Cancer Res*. 2008;68(10):3584-3590.

8. Baena E, Shao Z, Linn DE, et al. ETV1 directs androgen metabolism and confers aggressive prostate cancer in targeted mice and patients. *Genes Dev*. 2013;27(6):683-698.

9. Linn DE, Penney KL, Bronson RT, et al. Deletion of interstitial genes between TMPRSS2 and ERG promotes prostate cancer progression. *Cancer Res*. 2016;76(7):1869-1881.

10. Grasso CS, Wu YM, Robinson DR, et al. The mutational landscape of lethal castration-resistant prostate cancer. *Nature*. 2012;487(7406):239-243.

11. Sementchenko VI, Schweinfest CW, Papas TS, et al. ETS2 function is required to maintain the transformed state of human prostate cancer cells. *Oncogene*. 1998;17(22):2883-2888.

12. Carbone GM, Napoli S, Valentini A, et al. Triplex DNA-mediated downregulation of Ets2 expression results in growth inhibition and apoptosis in human prostate cancer cells. *Nucleic Acids Res*. 2004;32(14):4358-4367.

13. Robinson D, Van Allen EM, Wu YM, et al. Integrative clinical genomics of advanced prostate cancer. *Cell*. 2015;161 (5):1215-1228.

14. Wang L, Dehm SM, Hillman DW, et al. A prospective genome-wide study of prostate cancer metastases reveals association of wnt pathway activation and increased cell cycle proliferation with primary resistance to abiraterone acetate-prednisone. *Ann Oncol*. 2018;29(2):352-360.

15. Ross-Adams H, Lamb AD, Dunning MJ, et al.; CamCaP Study Group. Integration of copy number and transcriptomics provides risk stratification in prostate cancer: A discovery and validation cohort study. *EBioMedicine*. 2015;2(9):1133-1144.

16. Rayford W, Beksac AT, Alger J, et al. Comparative analysis of 1152 African-American and European-American men with prostate cancer identifies distinct genomic and immunological differences. *Commun Biol*. 2021;4(1):670.

17. Mertz KD, Setlur SR, Dhanasekaran SM, et al. Molecular characterization of TMPRSS2-ERG gene fusion in the NCI-H660 prostate cancer cell line: a new perspective for an old model. *Neoplasia*. 2007;9(3):200-206.

18. Corey E, Quinn JE, Buhler KR, et al. LuCaP 35: a new model of prostate cancer progression to androgen independence. *Prostate*. 2003;55(4):239-246.

19. Nguyen HM, Vessella RL, Morrissey C, et al. LuCaP prostate cancer patient-derived xenografts reflect the molecular heterogeneity of advanced disease an–d serve as models for evaluating cancer therapeutics. *Prostate*. 2017;77(6):654-671.

20. Wilson CG, Robert-Cooperman CE, Burkhardt BR. PANcreatic-DERived factor: novel hormone PANDERing to glucose regulation. *FEBS Lett*. 2011;585(14):2137-2143.

21. Wang C, Burkhardt BR, Guan Y, et al. Role of pancreatic-derived factor in type 2 diabetes: evidence from pancreatic beta cells and liver. *Nutr Rev*. 2012;70(2):100-106.

22. Moak SL, Dougan GC, MarElia CB, et al. Enhanced glucose tolerance in pancreatic-derived factor (PANDER) knockout C57BL/6 mice. *Dis Model Mech*. 2014;7(11):1307-1315.

23. Ellwood-Yen K, Graeber TG, Wongvipat J, et al. Myc-driven murine prostate cancer shares molecular features with human prostate tumors. *Cancer Cell*. 2003;4(3):223-238.

24. Sharma NV, Pellegrini KL, Ouellet V, et al. Identification of the transcription factor relationships associated with androgen deprivation therapy response and metastatic progression in prostate cancer. *Cancers (Basel)*. 2018;10(10):379.

25. Baumgart SJ, Nevedomskaya E, Lesche R, et al. Darolutamide antagonizes androgen signaling by blocking enhancer and super-enhancer activation. *Mol Oncol*. 2020;14(9):2022-2039.

26. Markowski MC, Wang H, Sullivan R, et al. A multicohort open-label phase II trial of bipolar androgen therapy in men with metastatic castration-resistant prostate cancer (RESTORE): a comparison of post-abiraterone versus post-enzalutamide cohorts. *Eur Urol*. 2021;79(5):692-699.

27. Stelloo S, Nevedomskaya E, Kim Y, et al. Integrative epigenetic taxonomy of primary prostate cancer. *Nat Commun*. 2018;9 (1):4900.

28. Pomerantz MM, Qiu X, Zhu Y, et al. Prostate cancer reactivates developmental epigenomic programs during metastatic progression. *Nat Genet*. 2020;52(8):790-799.

29. Vlaicu SI, Tegla CA, Cudrici CD, et al. Epigenetic modifications induced by RGC-32 in colon cancer. *Exp Mol Pathol*. 2010;88 (1):67-76.

30. Dai B, Kim O, Xie Y, et al. Tyrosine kinase Etk/BMX is up-regulated in human prostate cancer and its overexpression induces prostate intraepithelial neoplasia in mouse. *Cancer Res*. 2006;66(16):8058-8064.

31. Ye R, Cao C, Xue Y. Enhancer RNA: biogenesis, function, and regulation. *Essays Biochem*. 2020;64(6):883-894.

32. Ernst J, Kellis M. ChromHMM: automating chromatin-state discovery and characterization. *Nat Methods*. 2012;9 (3):215-216.

33. Wu D, Zhang C, Shen Y, et al. Androgen receptor-driven chromatin looping in prostate cancer. *Trends Endocrinol Metab*. 2011;22(12):474-480.

34. Ramanand SG, Chen Y, Yuan J, et al. The landscape of RNA polymerase -associated chromatin interactions in prostate cancer. *J Clin Invest*. 2020;130(8):3987-4005.

35. Zhang Z, Chng KR, Lingadahalli S, et al. An AR-ERG transcriptional signature defined by long-range chromatin interactomes in prostate cancer cells. *Genome Res*. 2019;29(2):223-235.

36. Arnold PR, Wells AD, Li XC. Diversity and emerging roles of enhancer RNA in regulation of gene expression and cell fate. *Front Cell Dev Biol*. 2019;7:377.

37. Cinghu S, Yang P, Kosak JP, et al. Intragenic enhancers attenuate host gene expression. *Mol Cell*. 2017;68(1):104-117.e6.

38. Johansson P, Bernstrom J, Gorman T, et al. FAM3B PANDER and FAM3C ILEI represent a distinct class of signaling molecules with a non-cytokine-like fold. *Structure*. 2013;21(2):306-313.

39. Kounatidou E, Nakjang S, McCracken SRC, et al. A novel CRISPR-engineered prostate cancer cell line defines the AR-V transcriptome and identifies PARP inhibitor sensitivities. *Nucleic Acids Res*. 2019;47(11):5634-5647.

40. Cao S, Zhan Y, Dong Y. Emerging data on androgen receptor splice variants in prostate cancer. *Endocr Relat Cancer*. 2016;23 (12):T199-T210.

41. Maciel-Silva P, Caldeira I, de Assis Santos I, et al. FAM3B/PANDER inhibits cell death and increases prostate tumor growth by modulating the expression of Bcl-2 and Bcl-XL cell survival genes. *BMC Cancer*. 2018;18(1):90.